

LASER INTERFEROMETER GRAVITATIONAL WAVE OBSERVATORY
- LIGO -
CALIFORNIA INSTITUTE OF TECHNOLOGY
MASSACHUSETTS INSTITUTE OF TECHNOLOGY

Technical Note	LIGO-T1100252-v2	2011/05/14
In Vacuum Beam Diverter		
J Fishner and S J Waldman		

California Institute of Technology
LIGO Project, MS 18-34
Pasadena, CA 91125
Phone (626) 395-2129
Fax (626) 304-9834
E-mail: info@ligo.caltech.edu

Massachusetts Institute of Technology
LIGO Project, Room NW22-295
Cambridge, MA 02139
Phone (617) 253-4824
Fax (617) 253-7014
E-mail: info@ligo.mit.edu

LIGO Hanford Observatory
Route 10, Mile Marker 2
Richland, WA 99352
Phone (509) 372-8106
Fax (509) 372-8137
E-mail: info@ligo.caltech.edu

LIGO Livingston Observatory
19100 LIGO Lane
Livingston, LA 70754
Phone (225) 686-3100
Fax (225) 686-7189
E-mail: info@ligo.caltech.edu

1 Introduction

The Advanced LIGO interferometers will have 10 times the phase sensitivity of the Initial LIGO interferometers over an extended frequency range. This corresponds to a 100x increase in the sensitivity to scattered power at each of the interferometer ports. Initial LIGO was sensitive to scattered light from the in-air optical tables at the AntiSymmetric (AS) port, End Test Mass (ETM) transmission, Reflection port (REFL), and Pick Off (PO) ports. To reduce this sensitivity, all the sensitive beams will be terminated on in-vacuum beam dumps during science mode. To maintain the capability to look at the beams on in-air optical tables during lock acquisition, there is a moving mirror in the vacuum system to “close” laser ports. This moving mirror is known as the *in-vacuum beam diverter* and this note describes its development and testing.

References

- [1] *The Advanced LIGO ETM transmission monitor*; S J Waldman; T0900385-v7
- [2] *ISC Rotary Beam Diverter*; J. Fishner and S J Waldman; D1100642
- [3] *±10 A Driver*; R. Abbott; D020164

2 Rotary design

The Beam Diverter consists of a 2” high-reflectivity dielectric mirror mounted on a rotary armature. The rotor rotates around a horizontal axis through approximately 90 degrees, translating the mirror by 2” into the beam and reflecting it into a high quality beam dump. Two major components drive the design: the vacuum compatible axle and bearing and the vacuum compatible motor.

2.1 Vacuum compatible bearing

This design represents the third iteration of an in-vacuum design. The first iteration, a flexure based design, had limited rotation range and an inherent spring that was difficult to tolerance properly. The second iteration, a linear motor, relied on linear bearings that repeatedly failed after being cleaned for vacuum. This design, shown in Fig. 2, uses sapphire jewel bearings and a hardened steel rod to create a vacuum compatible rotation bearing. The bearings are supported radially by pre-aligned, matching counterbores in the two face plates, as shown. The axle is constrained longitudinally using shaft collars with a small spacing to reduce friction.

2.2 Rotary motor

The motor for the rotary mount is based on the armature motor in hard disk drives. As shown in Fig. 3, the coil is wound on the rotor with two radial segments (of equal length) and

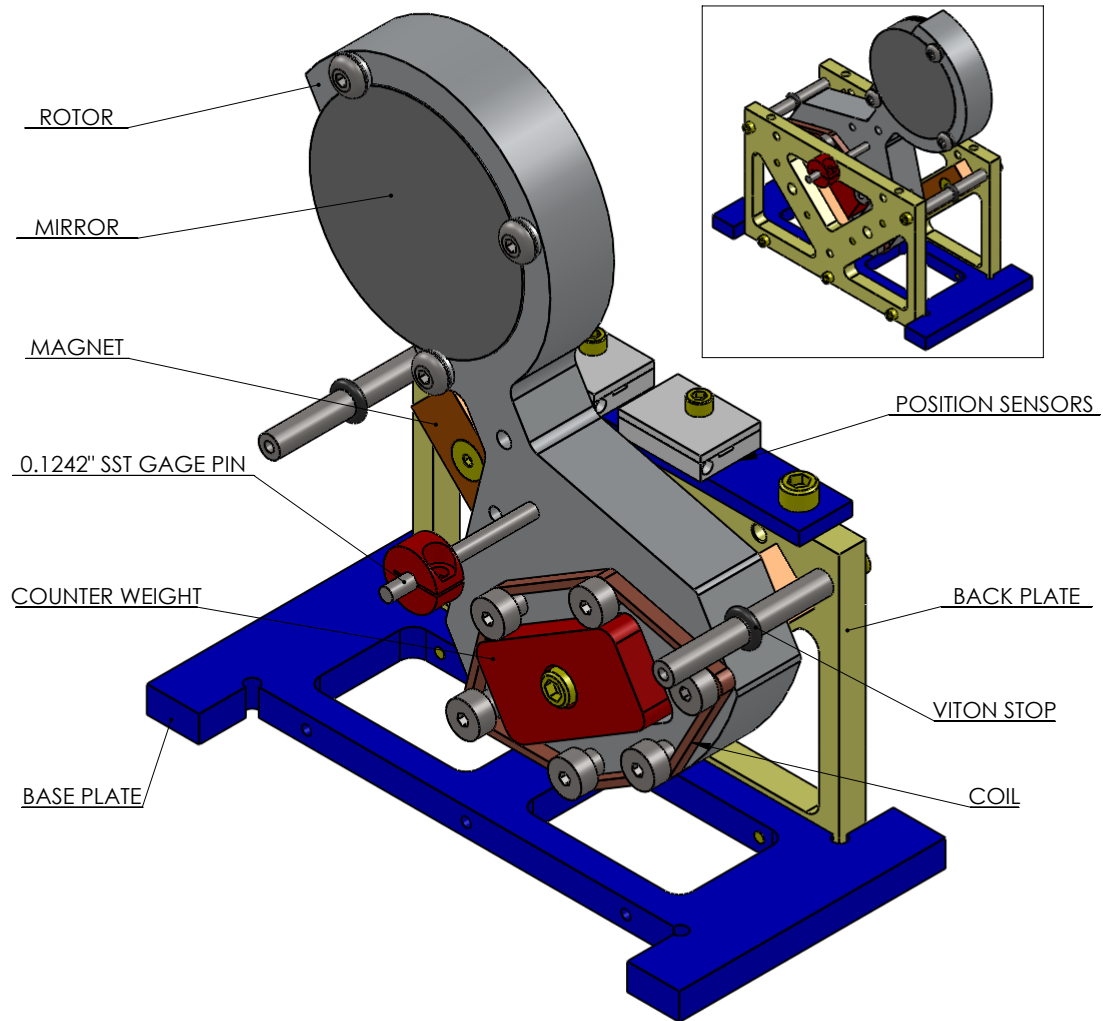


Figure 1: The rotary beam diverter design, with the mirror in both the closed position and the open position (inset). The front plate and magnets have been removed from the drawing for clarity.

two arc segments (one short and one long). The radial segments take the axis of rotation as their center. The magnets are arranged so that the field is concentrated at the radial segments and in opposite directions for each segment. Thus, the Lorentz force, $F = IL \times B$, for both radial segments is in the same direction and exerts a torque on the rotor. The coil is wound on stainless steel shoulder bolts using OSEM-like wire. The magnets are attached to magnetic stainless steel (410 or 416 alloys) that acts as a flux return for the field. The magnets are nickel coated NdFeB.

2.3 Balance, Limits and Sensing

The rotor's center of mass is located as close to and slightly above the axis of rotation. By minimizing the offset, we minimize the force required to overcome gravity. This also minimizes the shift of the center of mass between the open and closed positions and minimizes

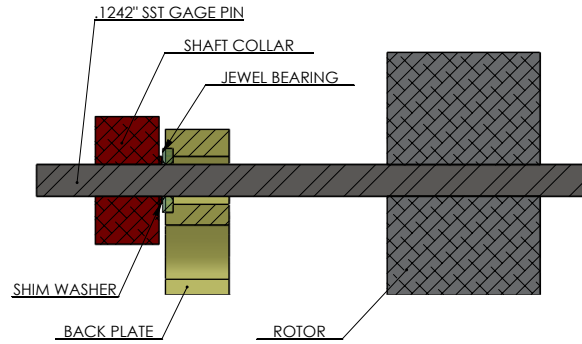


Figure 2: Design of the axle and bearing. A $\approx 0.005''$ gap is included between the shim washer and the shaft collar, set at assembly time.

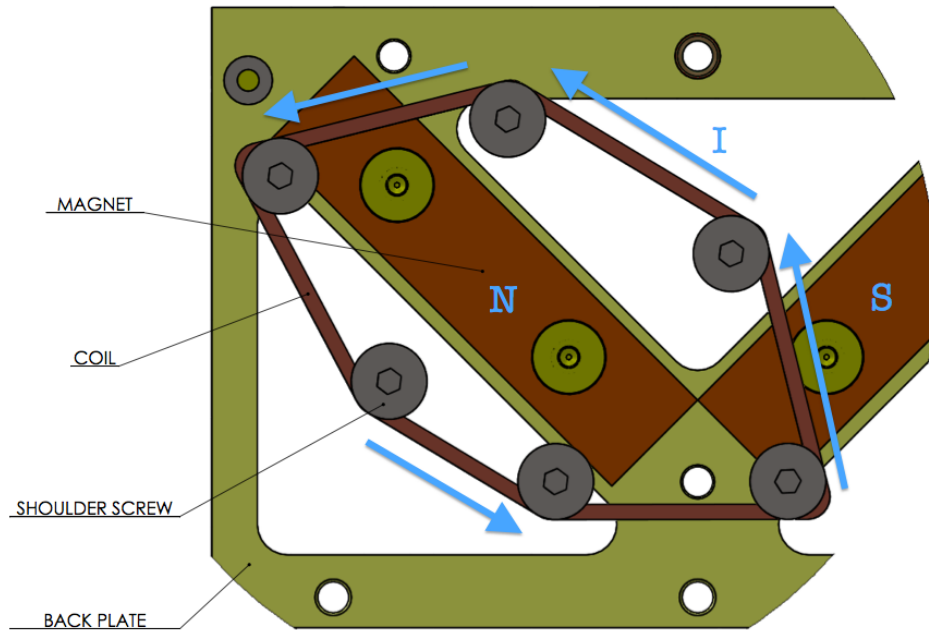


Figure 3: Design of the in-vacuum motor.

the back-reaction force exerted on the supporting table. By maintaining a small vertical offset, we ensure that there is a slight gravitational force pulling the rotor to the side against the stops. Altogether, we expect the rotor's 320 gram mass to shift by $500 \mu\text{m}$.

The rotor is stopped against two stainless steel standoffs. The mirror travels ± 30 degrees around the center line. The limits are set with Viton O-rings to limit the impulse.

As in all previous designs, the beam diverter has two "positive" sensors to confirm the rotor position as shown in Figure 4. The sensors are vacuum encapsulated magnetic reed relays that sense the location of a small magnet on the rotor. The sensors do not activate when the motor coil is energized. Consequently, they can be used to determine the required motor pulse duration and verify operation for each action. The sensors and the coil are wired to a Glenair connector mounted to a bracket on the rear plate.

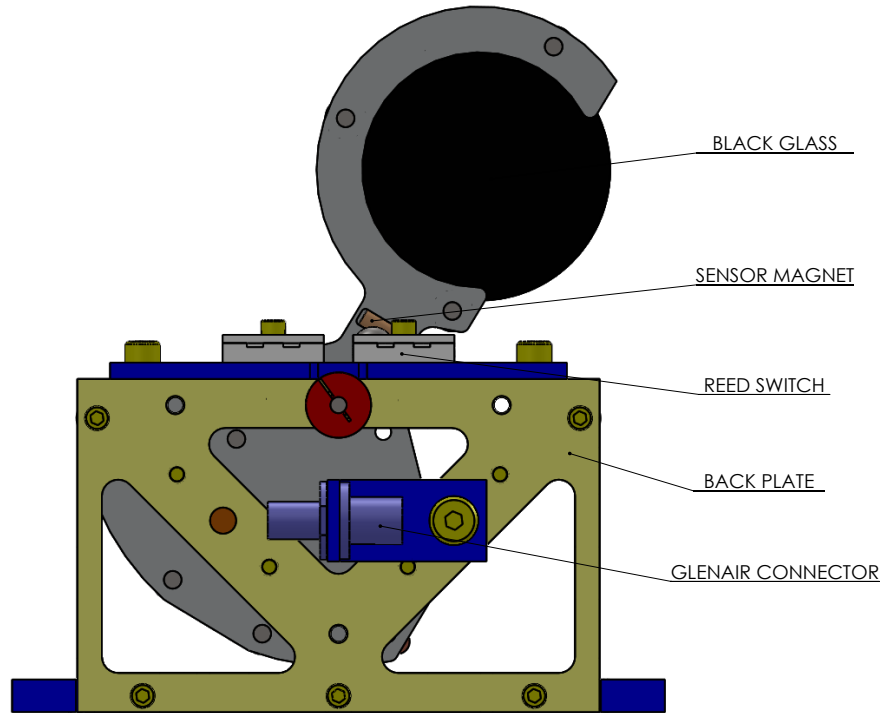


Figure 4: The position of the magnetic reed switch sensors, sensor magnet, and connector.

3 Assembly

3.1 Axle alignment

There are two critical assembly steps shown below: the alignment of the axle and jewel bearings and the spacing of the shaft collars. To reduce the alignment errors of the rotor with respect to the axle, the rotor is press fit onto the axle. To ensure good alignment between the jewel bearings, the side plates must be aligned to each other. As shown in Fig. 5, the plates are pre-aligned with two 0.125" rods set in slip-fit holes and fixed in place using the spacers.

Once the side plates are aligned to each other and the alignment rods removed, the jewel bearings are set in their counterbores (slip-fit) and the shaft collars attached. The shaft collars serve multiple purposes: they constrain the position of the rotor within the assembly, keep the jewel bearings in their counterbores, and act as a thrust bearing. To ensure smooth operation, a shim washer with a high quality finish is placed between the shaft collar and the jewel bearing. A small amount of play, about 5 mils, is ensured using a removable shim during assembly.

3.2 Coil winding

For the test prototype, 80 turns of 30 gauge in-vacuum wire (4.8 Ohms) is wound by hand around 6 stainless steel shoulder screws. No particular effort was made to ensure maximum density or to restrain the coils once in place. The coil leads are routed along the axle to

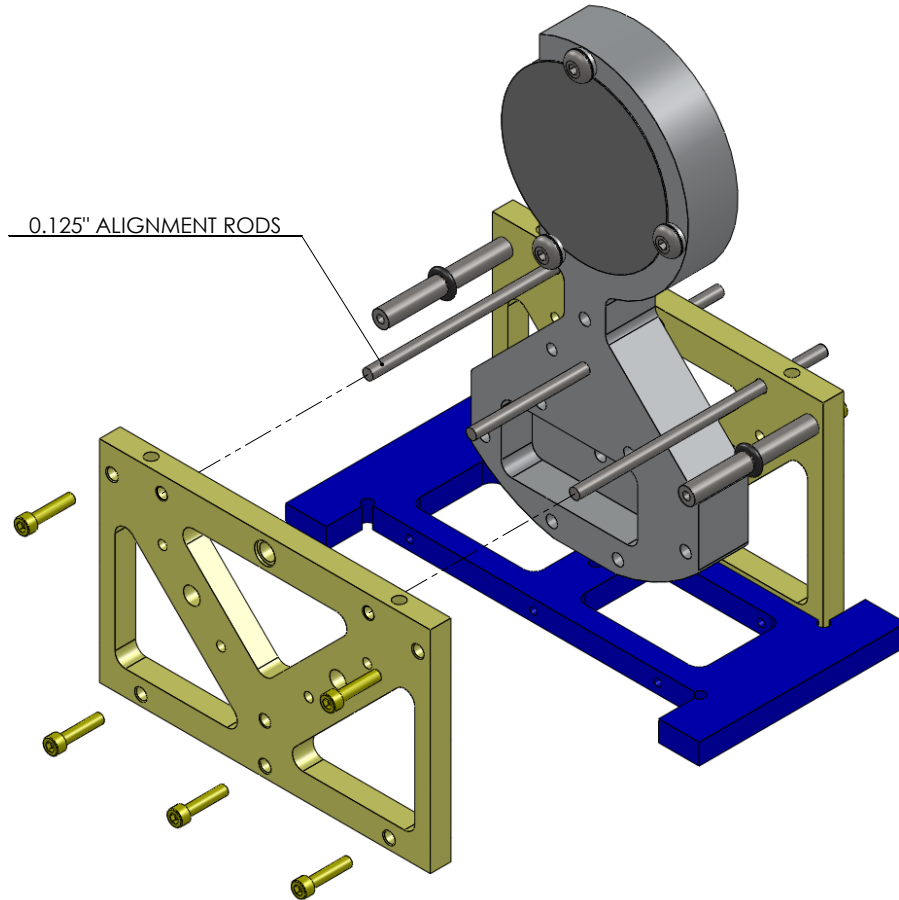


Figure 5: Alignment of the two side plates. The 0.125” rods are used to align the plates before bolting the assembly together. The rotor, magnets (not shown) and viton stops must be in place during alignment. After alignment, the guide rods are removed and the axle longitudinal position set with shaft collars.

minimize the torque they exert during the rotor’s motion. Anecdotal evidence suggests the wires exerted a force on the rotor and care should be made when dressing the wires to limit the applied spring.

At the nominal resistance of 100 Ohms/1000 ft, the 30 gauge prototype coil is 14.5 m long with each loop 18 cm long. The actual coil will be a 10 Ohm coil of MWS Industries 32HML, 32 gauge wire. This corresponds to 19 m of wire and roughly 100 turns of coil. For the same applied current, the real coil will require 20% less current, twice the applied voltage, and roughly 60% higher voltage, and 30% more power.

The production coil is expected to run with 250 mA, 2.5 V, and 0.6 W for approximately 2 seconds.

4 Testing

We performed a series of tests in vacuum and in air. The vacuum tests were performed in the Q-lab’s bell jar under a vacuum of approximately 5×10^{-4} torr. The coil was driven using a ± 10 A coil driver D020164 [3] running up to 670 mA of current. The coil driver is a voltage source, so we also recorded the coil current for every cycle. The beam diverter was tested for thermal performance, threshold currents, and for number of cycles. Given the improved axle and balance of the production units, we believe these tests represent worst case performance.

4.1 Thermal performance [in vacuum]

We operated the coil at 3 fixed applied voltages of 2 V, 3 V, and 4 V. For the nominal coil resistance of 6Ω , this corresponds to initial power of 330 mA, 500 mA, and 670 mA. For each input voltage, we measured the input voltage and current for 100 seconds. In all cases, the coil resistivity increased with a time constant of approximately 50 seconds. Assuming that the resistivity increase is entirely due to copper’s $0.4\%/K$ temperature coefficient, the change can be converted to a temperature as shown in Fig. 6. These data indicate a high

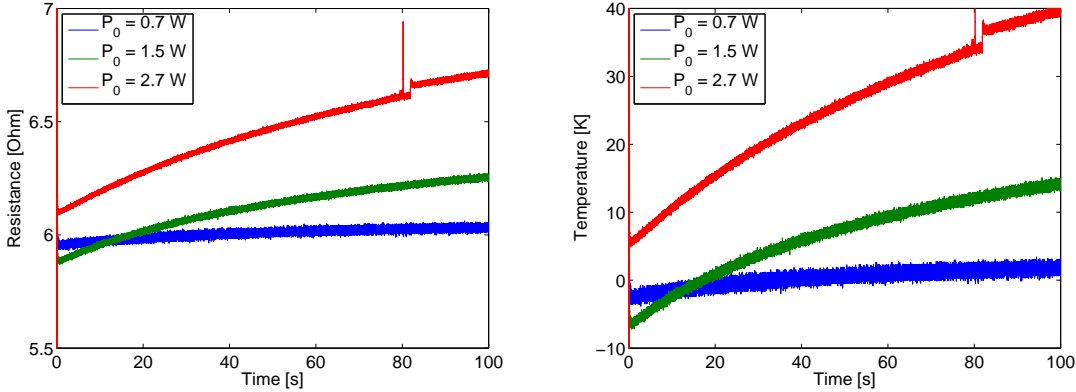


Figure 6: The coil resistance change over time for 3 applied voltages and the corresponding temperature change.

thermal impedance for the coil of $13 C/W$. For the expected power of 0.6 W, the steady state temperature rise will be 8 C. Including the 50 second thermal time constant and 2 second energization time, the actual temperature rise will be much less than 1 C.

4.2 10 thousand cycles [vacuum]

We ran the beam diverter in 4×10^{-4} torr vacuum for 10,500 cycles. For clockwise motion, we ran with 470 mA and for counter-clockwise motion 530 mA. The motor ran with a 50% duty cycle and an average power of 0.8 W. The drive algorithm was critical for reliability over long runs: run at constant voltage until the appropriate sensor triggers a successful transition, with a timeout at 5 seconds. With this algorithm, the motor successfully completed all but 1% of the cycles, with most of the failures from the counter-clockwise motion.

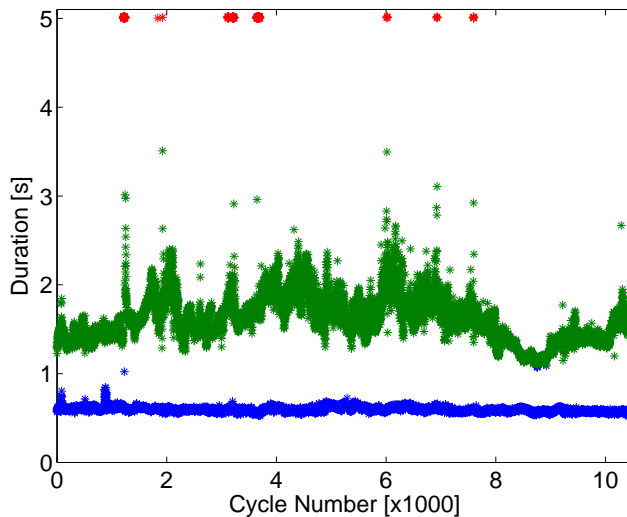


Figure 7: We ran the beam diverter in 4×10^{-4} torr vacuum for 10,500 cycles. For each cycle we recorded the time to move **clockwise**, **counter-clockwise**, and **failures**. Approximately 1% of the cycles failed, most moving counter-clockwise. The variation in counter-clockwise motion is believed to be caused by fluctuations in the axle's friction.

The variance in the duration of the counter-clockwise motion is indicative of the changing friction mentioned in the previous section. The greater time required is because of the offset in the center of mass. And the failures (defined here as a duration which times out after 5 seconds) all occur when the duration (and presumably the friction) is increasing.

We expect this term to decrease when an appropriate axle is used.

4.3 Threshold current [in vacuum, in air]

The prototype rotor was not correctly balanced. As a result, the rotor center of mass was located ≈ 20 degrees from the rotors vertical plane, above the axis. This created an asymmetry in the force and the time required to move clockwise versus counter clockwise. To establish a threshold, we measured time required for the rotor to move clockwise and counter-clockwise. Any motion that took longer than 5 seconds was considered a failure. This was repeated for a variety of control voltages and for each direction in vacuum and with the vacuum chamber vented. The results are shown in Figure 8.

At low drive currents, the required movement time is a function of the depth of the gravitational potential. At high drive currents, the rotor motion is slowed by the eddy current damping of the aluminum rotor moving through the magnetic field.

Moving to the left requires more than twice the force as moving to the right. This is believed to be entirely because of the rotor balancing, as described below. There is no apparent change between the in vacuum and in air threshold performance.

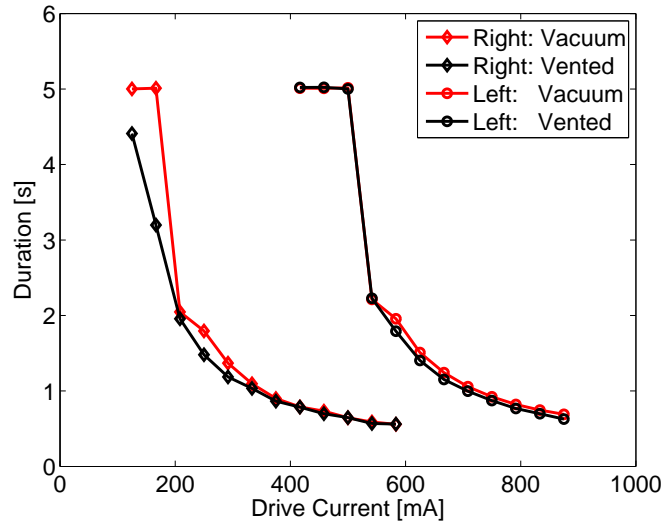


Figure 8: The threshold applied current for motion of the rotor to the right (diamonds) and to the left (circles). Measurements in vacuum and in air have the same threshold. The difference in current left vs. right is a result of the coil balance.

4.4 Improved axle [in air]

After completing the in vacuum tests, we removed the beam diverter from the chamber and replaced the axle. The original axle, labeled 0.125", was a 0.125" rod that had been sanded down with 400 grit sand paper to increase the clearance in the jewel bearing. The replacement axle is a 0.1242" precision gauge pin with a high quality surface finish. The difference in the threshold current is shown in Figure 9, and shows a slight decrease in the required drive for the better axle.

4.5 Improved balance [in air]

As mentioned before, the prototype beam diverter's rotor was incorrectly balanced, as reflected in the threshold drive. We adjusted the balance by taping an 8 gram bolt to the low-mass side of the diverter about 1 inch from the centerline. The center of mass was still above the axis of rotation. The results, shown in Figure 10, show that the required force is almost symmetric for clockwise versus counter-clockwise motion. As the center of mass moves closer to the axis for the production unit, we expect the required drive to decrease.

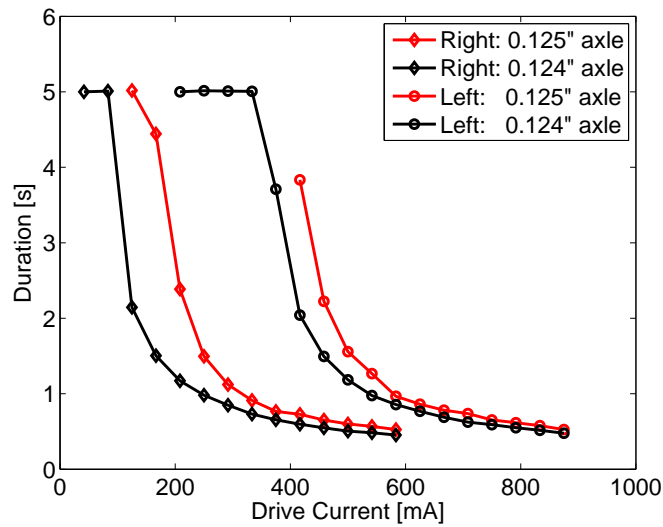


Figure 9: The threshold applied current for motion of the rotor to the right (diamonds) and to the left (circles) for two different axles. The 0.124" axle has a better surface finish and is slightly smaller diameter.

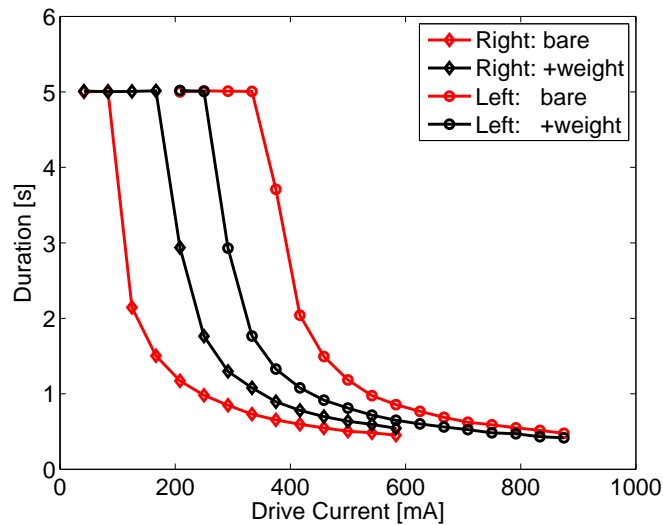


Figure 10: The threshold applied current for motion of the rotor to the right (diamonds) and to the left (circles) for two different counterweights. The addition of 8 grams of mass approximately 1" from the centerline balances the force.

5 Modifications for production unit

The tests performed above are intended to reflect the changes made to the production unit. To summarize the changes, they are:

- High finish 0.124" axle instead of 0.125" sanded axle,
- Improved balance and center of mass position, and
- Use of 32 gauge wire as in the OSEMs.

These changes are expected to reduce performance variation, lower the required drive, and fulfill the LIGO vacuum requirements.